Glider Flight Environment Modeling for Optimal Control

Dhaval D. Shah, Amor A. Menezes and Ilya V. Kolmanovsky

***Abstract*— This paper describes the process of creating a computationally-inexpensive yet relatively accurate atmospheric environment model for use in stochastic optimal control problems for glider flight management. In such problems, estimates of transition probabilities between flight in updrafts, downdrafts and thermals of varying strength are needed. This work proposes an atmospheric environment model that predicts updraft and downdraft strengths in a given region and, when combined with existing glider flight data, estimates thermal locations and strengths. The resultant predictions can be utilized to compute the desired transition probabilities. A simple approach currently employed in flight simulator games is adapted for updraft and downdraft modeling. The method is empirical and requires the computation of a linear factor. Interestingly, when validated against actual flight data, this technique is 92.4 percent accurate on average. This paper also shows that the location and intensity of thermals can be deduced from flight data by utilizing updraft and downdraft predictions. The work then illustrates the modeling process for a sample topographical area, and utilizes the model to solve a stochastic drift counteraction optimal control problem where control policies that maximize glider flight range are generated.**

I. Introduction

A. Motivation and Goals

Glider aircraft fly in an uncertain environment. This uncertainty is due to a lack of *a priori* knowledge of the locations and strengths of updrafts, thermals and downdrafts in the immediate flight environment. Updrafts are caused by the upward deflection of the prevalent wind over raised ground. Thermals are columns of rising air at lower altitudes of the Earth's atmosphere that are caused by uneven heating of the ground surface. Downdrafts (or sink) occur on the leeward side of raised ground deflecting the prevalent wind, and when air flows to the base of a nearby thermal. Exploiting the lift produced by updrafts and thermals, and either avoiding or minimizing the time spent in downdrafts, extends flight time and range. To facilitate the optimization of glider flight management decisions that accomplish this flight extension task, the flight environment (i.e., the updrafts, downdrafts and thermals) needs to be modeled.

Modeling the atmospheric environment to predict the locations and intensity of updrafts, downdrafts and thermals is a challenging problem that is also time-varying due to a dependence on changing wind speed and direction, time of day, and weather conditions. However, it is possible to utilize aggregated information about the glider flight environment. For instance, the Stochastic Drift Counteraction Optimal Control (SDCOC) approach proposed in [1] is based on representing the atmospheric environment by transition probability models. These transition probabilities predict the conditional probabilities of updraft, downdraft and thermal strength in the next flight segment given measured updraft, downdraft and thermal strength in the current flight segment. Such transition probabilities provide a simple approach that captures aggregate information about the flight environment for best on-average performance.

The objective of the present paper is to demonstrate how transition probabilities can be constructed for a given region based on a simple model of topographic lift and recorded flight data. We then illustrate the use of the constructed transition probabilities to produce a stochastic control policy for glider flight management.

B. Technical Approach and Related Literature

Traditional techniques to model updrafts and downdrafts consider a given region as a fixed three-dimensional volume, and calculate the interacting fluid flow at each and every point in that volume subject to boundary conditions. These calculations involve solving the Navier-Stokes equations within the volume, which is a task that is computationally expensive and difficult to implement within a stochastic control scheme.

This paper adapts an approach described in [2] to model updrafts and downdrafts based on a representation of topographic lift. The updraft or downdraft intensity due to the land topography is simulated by sampling the ground elevation of the terrain in a windward direction relative to the current position of the aircraft. The method has the advantage of being computationally simple, and, as we establish by comparing topographic lift to measured updraft data, is remarkably accurate. This updraft model can then be used to determine the location and intensity of thermals from previously recorded flight data, if available. The resultant stochastic models for updrafts and thermals can be utilized by SDCOC or any other stochastic control method for glider flight management in an uncertain environment.

Previous work on topographic flow can be found in [3]–[7]. These techniques solve a fluid flow problem and estimate the horizontal component of wind velocity over a hill. For the optimal control problem of interest in this paper, the vertical component of wind velocity needs to be estimated. We show that a simple model based on [2] provides this component with good accuracy.

Thermals are difficult to model due to their somewhat random appearance over various land features such as roads,

D. D. Shah and I. V. Kolmanovsky are with the Department of Aerospace Engineering, University of Michigan, Ann Arbor, MI 48109, USA. A. A. Menezes is with the Department of Bioengineering, University of California, Berkeley, CA 94720, USA. ddshah@umich.edu; amenezes@berkeley.edu; ilya@umich.edu

developed cities and ploughed fields, and their variable intensities that are dependent on the time of day and weather conditions (e.g., thermals are more common on bright sunny days than overcast days). Traditionally, thermal intensity is modeled empirically using information obtained from flight sensors and environment conditions, or by observing birds [8]–[13]. However, the thermals predicted by these models do not incorporate thermal intensity changes as a function of wind speed. Additionally, these models do not predict the presence of sink caused by thermals. In this paper, estimates of thermal and sink intensity are provided that include these factors.

The control framework employed in this paper is that of SDCOC [1], [14]. In SDCOC, a cost function is utilized that reflects the expected time to violate specified constraints and/or the expected total yield before violation of specified constraints. This control framework is of a dynamic programming type [15], but is different from average cost or discounted factor approaches.

C. Paper Outline

The remainder of this paper is as follows. Section II describes and validates our updraft and thermal modeling approach. Section III outlines the applicable theory for the SDCOC control law, and illustrates the use of this model in a glider range maximization problem. Lastly, Section IV presents concluding remarks.

II. Modeling of Flight Environment

A. Updraft and Downdraft Modeling

The essence of the flight simulation technique [2] is to continuously sample the ground elevation upwind of the aircraft and calculate slopes. This, combined with the wind strength and direction, produces a lift factor that can be applied to the glider. The ground elevation profile can be obtained over any land region using Google Earth. Since we consider low and moderately high wind-speeds (less than 50 knots), we assume that the wind flow is balanced (i.e., vortexes do not exist on the leeward side raised ground) and therefore neglect the effect of vortexes on the estimated updraft value.

This method requires five samples or probes of the ground elevation relative to the glider, and also takes the wind speed and direction as inputs. The slope at each of the probe points is used to compute an updraft value at the glider's location. The probes selected are as follows [2].

1) Probe zero: Located below the glider. Slopes from each of the other probes to the ground elevation at this point are calculated.
2) Probe one: Located 500 m upwind of the glider. The slope from probe zero to probe one is used to adjust the lift generated by the main slope calculated with probe two. Lift is increased if the upwind slope is concave, and reduced if the upwind slope is convex.
3) Probe two: Located 1000 m upwind of the glider. The slope from probe zero to probe two is the primary component of the lift factor for the glider.
4) Probe three: Located 3000 m upwind of the user glider. The slope from probe zero to probe three is used to detect high upwind ground elevations that adversely affect lift.
5) Probe four: Located 500 m downwind of the user glider. If the upward or downward slope continues behind or downwind of the glider then the main lift or sink is enhanced, but if the slope downwind is not in the same direction as the primary slope, the lift factor is reduced.

The ground elevations aligned into wind at 0 m, 500 m, 1000 m, 3000 m and -500 m with respect to the current glider location are denoted as $ge(0)$, $ge(1)$, $ge(2)$, $ge(3)$ and $ge(4)$ [meters], and the corresponding distances are denoted as $d(0)=0$, $d(1)$, $d(2)$, $d(3)$ and $d(4)$ [meters], respectively. The wind speed is denoted by v. We calculate slopes using:

$$slope(i-1) = \frac{ge(i)-ge(0)}{d(i)},\ i=1,2,3 \tag{1}$$

$$slope(4) = \frac{ge(4)-ge(0)}{d(4)}, \tag{2}$$

where $slope(1)$ is the primary determinant of the updraft at the current glider location [2]. A slope adjustment factor,

$$aslope(i) = \frac{\text{atan}(4\times slope(i))}{2},\ i=0,1,2,4, \tag{3}$$

is employed to "enhance gentle slopes, attenuate steep slopes, and smoothly limit values to between plus and minus 0.78 (i.e., $\pi/4$)" [2]. More empirically accurate distances at which to probe as well as updated slope calculation methods and slope adjustment functions are available in [2]; we utilize the original methodology here to baseline the results.

The value of $aslope$ for each $slope$ yields a lift factor, $factor(i)$, that corresponds to $aslope(i)$, $i=0,1,2,4$ [2]:

$$factor(0) = (aslope(1)-aslope(0))|factor(1)|, \tag{4}$$

$$factor(1) = -aslope(1), \tag{5}$$

$$factor(2) = \frac{-aslope(2)}{1.5}, \tag{6}$$

$$factor(4) = \frac{-aslope(4)}{4}, \tag{7}$$

where $factor(0)$ is the adjustment for a convex or concave slope, $factor(1)$ is the primary component of the lift, $factor(2)$ is the adjustment due to high or low ground 3000m upwind of the glider, and $factor(4)$ is the adjustment due to rising or falling ground 500m downwind of the glider. The total updraft value, U is given by

$$U = v\left(\sum_{i=0,1,2,4} factor(i)\right). \tag{8}$$

Again, empirical adjustments to the above equations for greater accuracy are available in [2].

The model based on the above expressions was implemented and tested over a region in Warner Springs, California. The elevation profile and updraft values computed for a single flight path over the region are shown in Fig. 1. The wind speed here is 20 knots flowing from left to right in the figure, and the flight path is in the same direction.

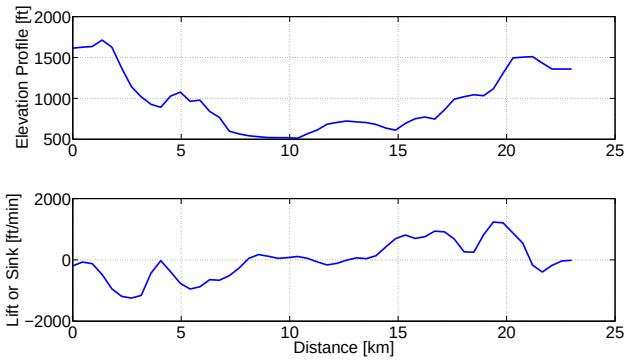

Fig. 1. Elevation and updraft profiles for a single flight path over the Warner Springs, CA region with a wind speed of 20 knots.

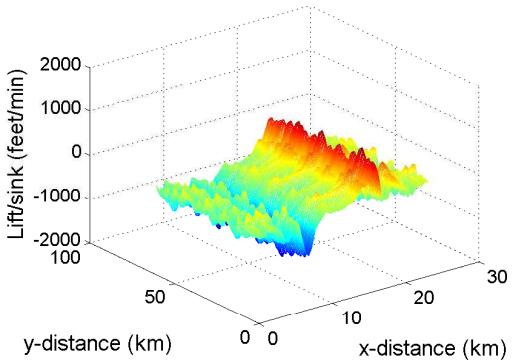

(a) Wind from 350 degrees.

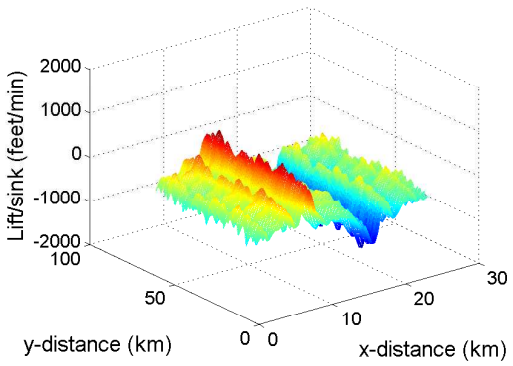

(b) Wind from 170 degrees.

Fig. 2. Updraft profile for the Warner Springs, CA region with a wind speed of 20 knots and direction as labeled.

The technique from [2] was extended so that updraft and downdraft profiles could be computed over two-dimensional regions, while accounting for wind components in various directions. Specifically, this involved the computation of multiple flight paths over a two dimensional grid. The Warner Springs area under consideration was a grid of 23 km $\times$ 61 km, which was divided into 14 paths. After resolving the wind speed and direction into its components, the updraft or downdraft along each of the 14 paths was computed and thereafter interpolated within the grid to find the updraft profile over the entire region. Sample results are presented in Fig. 2. Therefore, given any land terrain, wind speed and wind direction, estimates of the values of updraft and downdraft over the given region can be provided. Binning and counting the various updraft and downdraft values in the four cardinal directions yields updraft and downdraft transition probabilities for the associated region.

The results in Fig. 2 are intuitive since the windward side of every hill experiences lift and the leeward side experiences sink in proportion to the wind speed. When the wind direction is reversed, the positions of updrafts and downdrafts are interchanged. From (8), the magnitudes of updrafts and downdrafts are proportional to the wind speed.

The described approach to estimating updrafts has the following advantages:

1) An updraft and downdraft value can be ascertained for every point on a given landscape.
2) The updraft and downdraft profile is sensitive to local hillside contours.
3) The updraft and downdraft calculation is very simple and computationally efficient.

Interestingly, this simple updraft model also appears to be relatively accurate, as described below.

B. Validation of the Updraft and Downdraft Model

The updraft and downdraft model described in the previous section was validated using available flight data. (The original technique of [2], even for single flight paths, had never been formally validated with published results.) This flight data contained recorded glider flight path latitude and longitude coordinates, glider altitude at regular time instants along the flight path, and thermal locations as experienced by numerous gliders and glider types in various regions of the USA. A Vertical Speed Indicator (VSI) reading was generated from these data measurements for 10 different paths in the Warner Springs region. Each VSI reading was an interpretation of the combined effect of thermals and updrafts; however, the effect of thermals could be removed from calculated VSI readings by utilizing the recorded thermal data at appropriate flight path locations.

A resultant VSI profile and calculated updraft profile for the same flight path are shown in Fig. 3. It can be seen that the model is consistent with actual flight data. Table I indicates the mean error and standard deviation for 10 paths in the data. This technique is, overall, 92.4% accurate, with an average mean absolute percentage range error of 7.6%.

TABLE I

VALIDATION RESULTS FOR 10 FLIGHT PATHS

Path	Mean Percentage Absolute Range Error	Standard Deviation
1	10.29	6.32
2	10.53	6.27
3	8.01	5.19
4	6.68	4.86
5	4.48	4.2
6	4.69	2.77
7	6.40	4.06
8	12.3	7.03
9	5.61	3.67
10	6.95	5.05

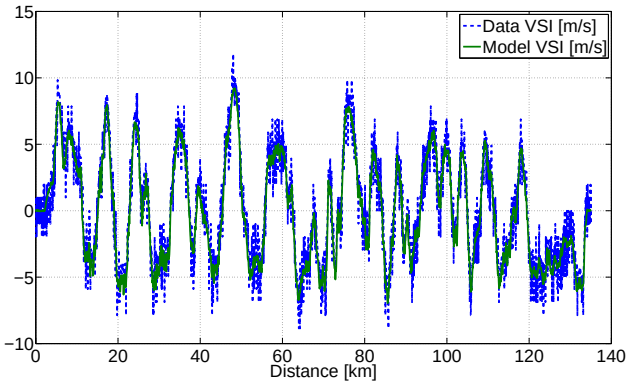

Fig. 3. A calculated non-thermal VSI profile and a modeled updraft profile.

C. Modeling and Validation of Thermals

The updraft/downdraft model together with available flight data were then used to determine the location and intensity of thermals in a given region. Various flight paths (that were unlike those used for validation) over the Warner Springs region were considered, and a VSI reading was obtained from the data set. The updrafts over the same region were computed using the model from the previous subsections, and the difference between the updraft and VSI readings from the flight data provided an estimate of thermal intensities. The thermal locations were estimated by considering locations of significant variation in the difference profile.

Fig. 4 shows the thermal intensity profile for the Warner Springs region obtained using this method. Twenty flight paths were used during an averaged time of day between 1800–1930 Coordinated Universal Time (UTC). We note the presence of "negative thermals," or locations of strong sink. In practice, the land that is located around a thermal experiences sink due to air flow rushing to the base of the thermal to replace rising air. Hence, the formation of thermal-like sinks with negative intensity values.

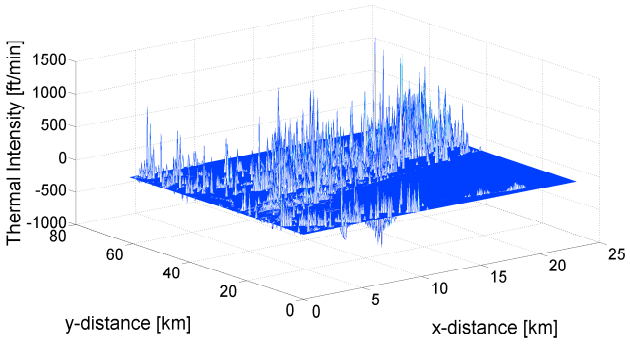

Fig. 4. Thermal intensity profile over the Warner Springs region.

It was also observed that when the grid size was reduced to 100 m, the generated thermal profile was discrete enough that a thermal encountered during different flight paths at the same time of day on different days at roughly the same location had the same intensity.

As before, binning and counting the various lift and sink values in the four cardinal directions yielded thermal transition probabilities for the Warner Springs region.

Validation of the above approach was completed using existing flight data from [16] and a software package called SEEYOU, which is used by soaring pilots to view their flights. This software provides the location and intensity of a thermal based on flight data. The thermal profile generated for the Warner Springs region with our approach was compared with the locations of thermals obtained from the software. It was observed that the locations of thermals from the software and the model were exactly the same. Moreover, encountering what is essentially the same thermal over multiple flight paths and obtaining the same intensity served as another validation mechanism.

Remark: The thermal locations and intensities obtained using either our approach or from SEEYOU with existing flight data can be correlated to land cover classifications over the same region. The resulting model can give a probabilistic estimate of thermal intensities over any land cover classification, and this extended model will not depend on having readily available, region-specific flight data corresponding to the place where the stochastic control technique is to be applied. Such an extended model is left to future work.

III. Glider Control Application

A. Range Maximization Model

The glider used for this application is Schweizer Aircraft's SGS 2-33A, details of which are given in [17], [18]. We assume that the glider flight path is partitioned into segments, and we let Δs denote the distance of a single flight segment. In each flight segment, the glider can encounter a thermal with strength (altitude increase rate) w_2, and the glider can spend u_2 seconds climbing this thermal. We also assume that the glider flies each flight segment with longitudinal speed u_1 when outside the thermal. This results in the altitude change rate $(f(u_1)+w_1)$, where $f(u_1)$ is the the polar curve representing the sink rate of the glider in still air given the glider longitudinal speed u_1, and w_1 denotes the time rate of change of the altitude due to the updraft (or downdraft, if w_1 is negative). The polar curve of the glider is described by a quadratic function of the longitudinal speed u_1 of the glider, $v_z[\text{ft/sec}] = 8.2582 - 0.2870u_1[\text{mph}] + 0.0038u_1[\text{mph}]^2$.

The following update equations approximately model the glider's flight:

$$h^+ = h + (-f(u_1) + w_1)\frac{\Delta s}{u_1} + w_2 u_2, \tag{9}$$

$$t^+ = t + u_2 + \frac{\Delta s}{u_1}, \tag{10}$$

where h is the altitude at the start of a flight segment, t is the total time traveled prior to the start of the flight segment, h^+ is the altitude at the end of the flight segment, and s^+ is the total time traveled at the end of the flight segment. The variables u_1 and u_2 are control variables.

A Markov chain model is used to describe the evolution of thermal strength and updraft strength along the flight path, which enables us to predict the probability of encountering

a thermal and updraft of a given intensity in the next flight segment given the intensity of the thermal and updraft encountered in the current flight segment.

The objective of the stochastic range maximization problem is to determine a control law that maximizes the expected distance that the glider can travel within a given time, t_{max}, i.e., the expected distance that the glider can travel before the system states exit a prescribed set,

$$G = \{(h,t) : \ h_{min} \leq h \leq h_{max}, \ t \leq t_{max}\}. \tag{11}$$

The flight path in this case was assumed to be a one-dimensional path over the two-dimensional region. Updrafts/downdrafts and thermals along this path were generated using their respective transition probabilities.

B. SDCOC Law Computation

Our objective is to determine a control function $u(x,w)$, such that with $v(t) = u(x(t),w(t))$, a cost functional of the form,

$$J^{x_0,w_0,u} = \mathrm{E}_{x_0,w_0}[\tau^{x_0,w_0,u}(G)], \tag{12}$$

is maximized. Here, $\tau^{x_0,w_0,u}(G) \in \mathbb{Z}^+$ represents the first-time instant when the trajectory of $x(t)$ and $w(t)$, which is denoted by $\{x^u, w^u\}$, resulting from the application of the control $v(t) = u(x(t),w(t))$ with values in the set U exits the prescribed compact set G.

The details of the SDCOC technique are described in [1].

For the range maximization problem, the minimum and maximum altitudes for the glider were selected as $h_{min} =$ 1000 ft and $h_{max} = 5000$ ft. For the value iterations, the altitude grid had a step size of 100 ft, $t_{min} = 0$ s, $t_{max} = 1200$ s, and a grid step size of 30 s. The updraft grid was selected from -200 ft/min to 500 ft/min with a step size of 100 ft/min. The thermal grid was from -200 ft/min to 700 ft/min with a step size of 100 ft/min. All values of updrafts and thermals were rounded to a grid point. Both these grids were treated independent of each other. The rounded transition probabilities for the thermals P_t and updrafts P_u are given in (13) and (14), respectively. Due to rounding, the rows may not sum to 1 exactly.

$$P_t = \begin{bmatrix} 0.21 & 0.12 & 0.66 & 0 & 0 & 0 & 0 & 0 & 0 & 0 \\ 0.03 & 0.29 & 0.66 & 0.02 & 0 & 0 & 0 & 0 & 0 & 0 \\ 0 & 0 & 0.98 & 0.01 & 0 & 0 & 0 & 0 & 0 & 0 \\ 0 & 0.01 & 0.67 & 0.26 & 0.03 & 0.01 & 0.01 & 0 & 0 & 0 \\ 0 & 0.01 & 0.74 & 0.1 & 0.08 & 0.03 & 0.01 & 0.01 & 0 & 0.01 \\ 0 & 0.01 & 0.78 & 0.05 & 0.05 & 0.06 & 0.02 & 0.01 & 0 & 0.01 \\ 0 & 0.01 & 0.8 & 0.06 & 0.03 & 0.04 & 0.03 & 0.01 & 0.01 & 0.01 \\ 0 & 0.01 & 0.81 & 0.04 & 0.05 & 0.02 & 0.02 & 0.02 & 0.01 & 0.02 \\ 0 & 0.01 & 0.79 & 0.06 & 0.03 & 0.02 & 0.02 & 0.01 & 0.02 & 0.03 \\ 0 & 0.01 & 0.82 & 0.04 & 0.02 & 0.02 & 0.01 & 0.02 & 0.02 & 0.04 \end{bmatrix}, \tag{13}$$

$$P_u = \begin{bmatrix} 0.95 & 0.05 & 0 & 0 & 0 & 0 & 0 & 0 \\ 0.07 & 0.82 & 0.1 & 0 & 0 & 0 & 0 & 0 \\ 0 & 0.07 & 0.85 & 0.08 & 0 & 0 & 0 & 0 \\ 0 & 0 & 0.12 & 0.8 & 0.08 & 0 & 0 & 0 \\ 0 & 0 & 0.01 & 0.14 & 0.75 & 0.1 & 0 & 0 \\ 0 & 0 & 0 & 0.01 & 0.16 & 0.72 & 0.11 & 0 \\ 0 & 0 & 0 & 0 & 0.02 & 0.17 & 0.65 & 0.16 \\ 0 & 0 & 0 & 0 & 0 & 0.01 & 0.06 & 0.93 \end{bmatrix}. \tag{14}$$

The thermal and updraft grids were selected based on the authors' flying experience and the flight data VSI readings. This also allowed comparisons between thermal and updraft profiles over different regions. The transition probabilities that were generated were independent of flight direction because the probability of transitioning from one lift value to another was calculated based on the updrafts and thermals encountered in the four principal directions at each grid point. The grid for u_1 was selected as 39, 42, 45, 48, 54, 60, 66, 72, 78, 84, 90 mph and the grid for u_2 was selected as 0, 30, 60, 120, 180, 240, 300 s.

C. Range Maximization Results

Fig. 5 illustrates the convergence of the value function in the range maximization problem for zero values of updrafts and thermals. Fig. 6 illustrates cross-sections of the control policy for thermals of 400 ft/min and updrafts of 200 ft/min.

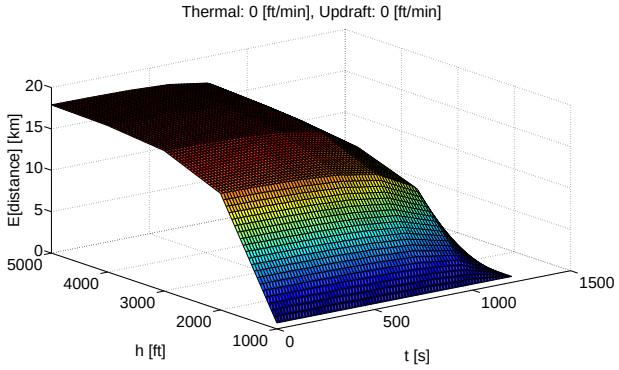

Fig. 5. Value function in the range maximization problem.

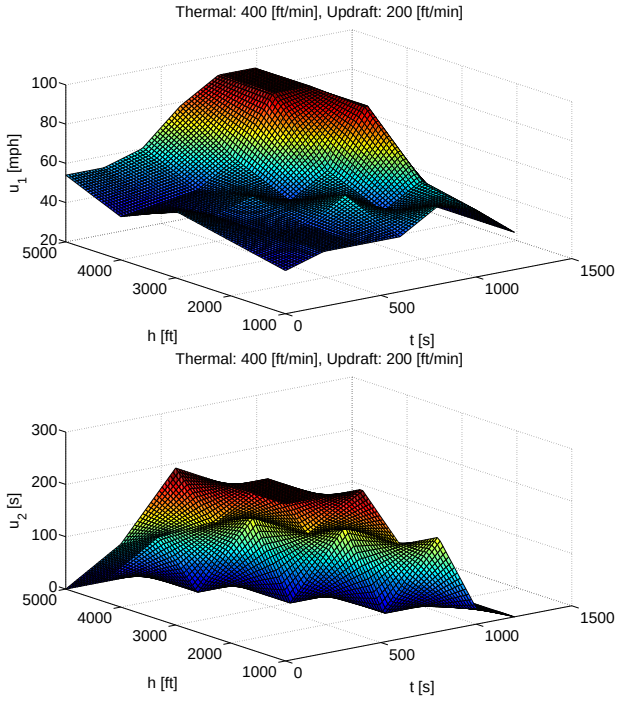

Fig. 6. Cross-sections of the control policy.

The trends seen in the control policy are somewhat consistent with the general rules-of-thumb that are taught to glider student pilots for range maximization (see [1]). Figs. 7–9 illustrate the time histories of the associated variables for a simulation scenario with an initial altitude of 2000 ft, initial thermal intensity of 200 ft/min and initial updraft intensity of 200 ft/min. The red dashed lines indicate constraints, and the blue lines indicate snapshots of flight conditions during flight segments. The glider utilizes strong early thermals but skips thermals encountered later in the glide to avoid losing time. Early in the simulation, the glider travels faster through downdrafts to avoid losing altitude (e.g., between s = 4 km and 5.5 km), slower through updrafts to take advantage of the added lift (e.g., between s = 0 km and 1.5 km), and close to the best lift/drag longitudinal speed value in flight segments without updrafts or downdrafts (e.g., between s = 1.75 km and 2.5 km).

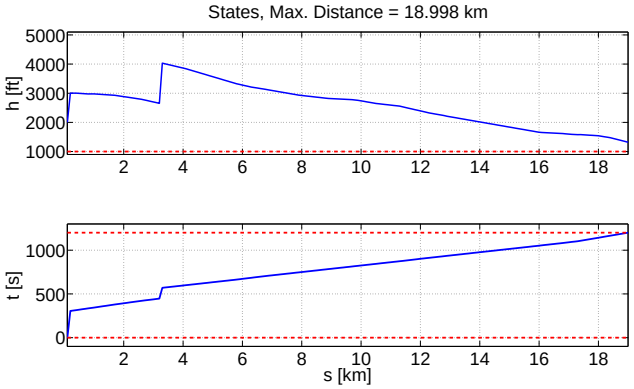

Fig. 7. Altitude and flight time of the glider versus distance.

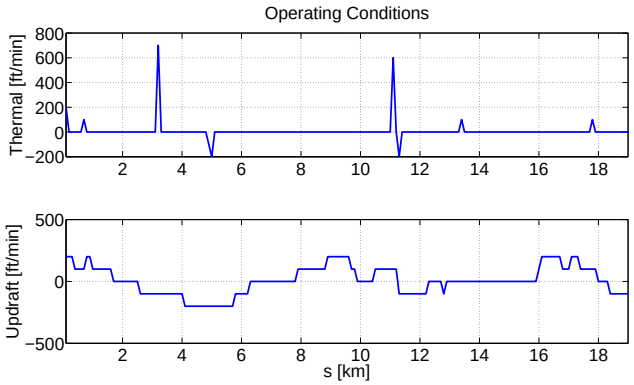

Fig. 8. Thermal strength and updraft versus distance

IV. Conclusions

This paper has proposed and verified a method to accurately model a glider's flight environment. The approach is computationally cost effective and easy to implement.

V. Acknowledgments

We are grateful for the valuable insights provided by Ian Forster-Lewis, who authored [2], the basis of this work.

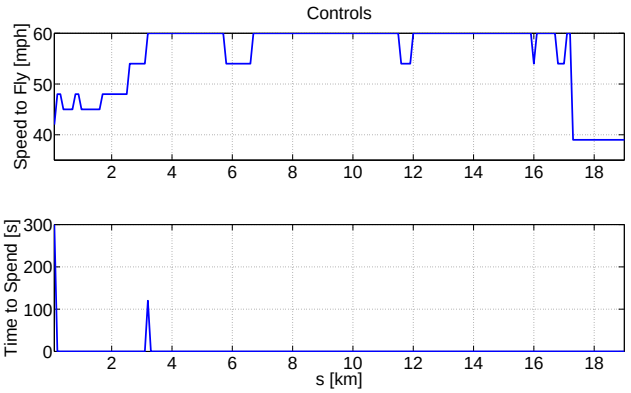

Fig. 9. Time to spend in a thermal and speed to fly versus time.

References

[1] I. V. Kolmanovsky and A. A. Menezes, "A stochastic drift counteraction optimal control approach to glider flight management," in *Proceedings of the 2011 American Control Conference*, 29 June–11 July 2011, pp. 1009–1014.

[2] I. Forster-Lewis, "Efficient simulation of topographic lift in microsoft flight simulator (fsx)," December 2007. [Online]. Available: http://carrier.csi.cam.ac.uk/forsterlewis/soaring/sim/fsx/dev/sim_probe/sim_probe_paper.html

[3] J. H. Cochrane, "MacCready theory with uncertain lift and limited altitude," *Technical Soaring*, vol. 23, pp. 88–96, July 1999.

[4] D. M. Deaves, "Wind over hills: A numerical approach," *Journal of Wind Engineering and Industrial Aerodynamics*, vol. 1, pp. 371–391, 1975.

[5] L. M. Paiva, G. C. Bodstein, and W. F. Menezes, "Numerical simulation of atmospheric boundary layer flow over isolated and vegetated hills using rams," *Journal of Wind Engineering and Industrial Aerodynamics*, vol. 97, pp. 439–454, November 2009.

[6] J. R. Pearse, "Wind flow over conical hills in a simulated atmospheric boundary layer," *Journal of Wind Engineering and Industrial Aerodynamics*, vol. 10, pp. 303–313, December 1982.

[7] M. Kobayashi, J. Pereira, and M. Siqueira, "Numerical study of the turbulent flow over and in a model forest on a 2d hill," *Journal of Wind Engineering and Industrial Aerodynamics*, vol. 53, pp. 357–374, 1994.

[8] Y. Leshem and Y. YomTov, "The use of thermals by soaring migrants," *Ibis*, vol. 138, pp. 667–674, 1996.

[9] F. Bernis, "Migration of falconiformes and *Ciconia* spp. through the straits of Gibraltar, part 2," *Ardeola*, vol. 21, pp. 489–580, 1980.

[10] M. J. Allen and V. Lin, "Guidance and control of an autonomous soaring vehicle with flight test results," in *Proceedings of the 45th AIAA Aerospace Sciences Meeting and Exhibit*, January 2007.

[11] L. S. Buurma, "Patterns of high bird migration over the North Sea area in October," *Limosa*, vol. 60, pp. 63–74, 1987.

[12] S. Christensen, O. Lou, M. Muller, and H. Wohlmuth, "The spring migration of raptors in southern Israel and Sinai," *Sandgrouse*, vol. 3, pp. 1–42, 1981.

[13] M. J. Allen, "Updraft model for development of autonomous soaring uninhabited air vehicles," in *Proceedings of the 44th AIAA Aerospace Sciences Meeting and Exhibit*, no. AIAA 2006-1510, January 2006.

[14] I. V. Kolmanovsky, L. Lezhnev, and T. L. Maizenberg, "Discrete-time drift counteraction stochastic optimal control: Theory and application-motivated examples," *Automatica*, vol. 44, pp. 177–184, January 2008.

[15] D. P. Bertsekas, *Dynamic Programming and Optimal Control*, 3rd ed. Athena Scientific, 2007, vol. I and II.

[16] [Online]. Available: http://www.onlinecontest.org/olc-2.0/gliding/flightsOfAirfield.htm

[17] *The 2-33 Sailplane Flight - Erection - Maintenance Manual*. Schweizer Aircraft Corporation.

[18] Department of National Defense, Canada, *Air Cadet Gliding Program Manual*, 2010, no. A-CR-CCP-242/PT-005.